



A Method for SRTM DEM Elevation Error Correction in Forested Areas Using ICESat-2 Data and Vegetation Classification Data

Yi Li , Haiqiang Fu *, Jianjun Zhu, Kefu Wu, Panfeng Yang, Li Wang and Shijuan Gao

School of Geoscience and Info-Physics, Central South University, Changsha 410083, China; fysjxsw@csu.edu.cn (Y.L.); jjz@csu.edu.cn (J.Z.); kefuwu@csu.edu.cn (K.W.); yangpanfeng@csu.edu.cn (P.Y.); wang9687@csu.edu.cn (L.W.); gaoshijuan@csu.edu.cn (S.G.)

* Correspondence: haiqiangfu@csu.edu.cn; Tel.: +86-731-88836931

Abstract: The past decade has witnessed the rapid development of the SRTM (Shuttle Radar Topography Mission) DEM (digital elevation model) in engineering applications and scientific research. The near-global SRTM DEM was generated based on radar interference theory. The latest version of the SRTM DEM with a resolution of 1 arc-second has been widely used in various applications. However, many studies have shown the poor elevation accuracy of the SRTM DEM in forested areas. Recent developments in the field of spaceborne lidar have provided an additional chance to correct the elevation error of the SRTM DEM in forested areas. We developed an easy-to-use method to correct the elevation error of the SRTM DEM based on the spatial interpolation method using the recent Ice, Cloud and land Elevation Satellite-2 data. First, an ICESat-2 terrain control point selection criterion was proposed to reject some erroneous ICESat-2 terrains caused by many factors. Second, we derived the elevation correction surface based on the interpolation method using the refined ICESat-2 terrain. Finally, a corrected SRTM DEM of forested areas was generated through the obtained elevation correction surface. The proposed method was tested in the typical forested area located in Massachusetts, USA. The results show that the RMSE of the selected terrain control points in vegetation areas and non-vegetation areas are 1.03 and 0.68 m, respectively. The corrected SRTM DEM have an RMSE of 4.2 m which is significantly less than that of the original SRTM DEM with an RMSE of 9.8 m, which demonstrates the proposed method is feasible to correct the elevation error in forested areas. It can be concluded that the proposed method obviously decreases the elevation error of the original SRTM DEM.

Keywords: SRTM DEM; ICESat-2 ATL08 products; vegetation classification data; interpolation methods; elevation correction surface



Citation: Li, Y.; Fu, H.; Zhu, J.; Wu, K.; Yang, P.; Wang, L.; Gao, S. A Method for SRTM DEM Elevation Error Correction in Forested Areas Using ICESat-2 Data and Vegetation Classification Data. *Remote Sens.* **2022**, *14*, 3380. <https://doi.org/10.3390/rs14143380>

Academic Editors: Zengyuan Li, Lin Cao and Erxue Chen

Received: 29 May 2022

Accepted: 11 July 2022

Published: 13 July 2022

Publisher's Note: MDPI stays neutral with regard to jurisdictional claims in published maps and institutional affiliations.



Copyright: © 2022 by the authors. Licensee MDPI, Basel, Switzerland. This article is an open access article distributed under the terms and conditions of the Creative Commons Attribution (CC BY) license (<https://creativecommons.org/licenses/by/4.0/>).

1. Introduction

A digital elevation model (DEM) presents 2.5-dimensional (2.5D) information of the Earth's surface. DEMs have a wide range of Earth disaster prevention [1,2], resource exploration [3,4], engineering construction [5,6], hydrological research [7,8], ecological protection [9], and forest monitoring [10]. DEMs are of interest because they have practical engineering applications and high scientific research value. The Shuttle Radar Terrain Mission (SRTM), sponsored by the National Geospatial-Intelligence Agency (NGA) and National Aeronautics and Space Administration (NASA), produced an unprecedented near-global DEM product. SRTM used two basic instruments: a C-band radar provided by the Jet Propulsion Laboratory (JPL) and an X-band radar provided by the German and Italian space agencies [11,12]. Studies have shown that the vertical and horizontal errors of the SRTM DEM are less than 20 m and 16 m, respectively, with 90% confidence, which is considered a relatively reliable DEM data source [13]. Moreover, the past decade

has seen the rapid development of SRTM DEMs in many applications, such as surface deformation [14,15], disaster monitoring [1,2], and hydrological surveys [7,8].

Generally, a high-accuracy SRTM DEM is essential for a wide range of scientific and engineering applications. The SRTM DEM shows high accuracy for uncovered terrain surfaces. However, due to the short wavelength, radar waves cannot penetrate the forest canopy cover to reach the land surface, so the SRTM DEM cannot reflect the subcanopy terrain [11]. There is a key limitation for many applications of the SRTM DEM, which is the poor elevation accuracy in forested areas [11]. The elevation error of the SRTM DEM in forested areas has received considerable critical attention. Therefore, what type of data is collected and what approach can be used to correct the elevation error of the SRTM DEM in forested areas has become a widely studied issue in the field.

As an active remote sensing approach, light detection and ranging (LiDAR) represents a significant data source to assess and correct the elevation errors of SRTM DEMs in forested areas. It can efficiently penetrate the gap in the trees thanks to the use of focused short-wavelength laser pulses. Studies over the past two decades suggest that fine-resolution DEMs with high accuracy in forested areas can be generated through LiDAR data [16]. Scholars have actively conducted research on LiDAR application to assess and correct DEMs in forested areas. Su et al. combined DTM derived from airborne LiDAR, vegetation structure features (such as canopy height, canopy cover, and vegetation index), and the parameters derived by DEM (such as slope and aspect) to correct the elevation errors of SRTM DEM in forested areas in California, USA. This approach significantly improved the elevation accuracy of the SRTM DEM in forested areas [17]. However, the vegetation structure features, and airborne LiDAR data are very limited, which limits the application of SRTM DEM correction in large-scale forested areas. To correct the elevation error of the SRTM DEM on a large scale, the space-borne lidar, Ice, Cloud, and land Elevation Satellite-1 (ICESat-1) was used due to near-global control point generation. Zhao et al. used the elevations derived from ICESat-1 data, combined with vegetation types, tree heights, terrains, vegetation coverage, and other data, to correct the elevation error of the SRTM DEM in vegetation areas on a global scale [18]. Loughlin et al. explored the functional relationship between the elevation error of the SRTM DEM and the forest vegetation coverage. The established functional relationship was used to correct the elevation error of the SRTM DEM on a global scale [19]. In addition, ICESat-1 was also used to correct the elevation error of the Advanced Spaceborne Thermal Emission and Reflection Radiometer Global Digital Elevation Model (ASTER GDEM) based on the moving average interpolation method [20]. Previous research has established that, in terms of the elevation error correction of the SRTM DEM in forested areas, the space-borne lidar mitigates the limitations of the SRTM DEM elevation error correction in a large-scale forested area. However, the Earth observation mission of ICESat-1 ended in 2009 and cannot continue to provide terrain control points for the elevation error correction of the SRTM DEM. During the mission, ICESat-1 had a low sampling rate, and the slope greatly prevented its usability, which limited its ability to correct the elevation errors of the SRTM DEM. In addition, the above methods for correcting the elevation error of the SRTM DEM required lots of input datasets and complex algorithm models.

Although ICESat-1 has been retired, investigations about the mission of the new generation of space-borne lidar (ICESat-2) need to be conducted. As the successor of ICESat-1, ICESat-2 is equipped with an Advanced Terrain Laser Altimeter System (ATLAS), which uses a new single-photon counting technique [21]. It can generate a dense spot along the track, while the spot diameter is small enough to resist the influence of the slope. In addition, it has a higher spatial resolution of 0.7 m than ICESat-1 [22]. The dense terrain control points provided by ICESat-2 make it possible to correct the elevation error of the SRTM DEM based on an easy-to-use method. Recent developments in the field of space-borne lidar have led to renewed interest in the elevation error correction of the SRTM DEM. Therefore, we developed an easy-to-use method for the elevation error correction of the SRTM DEM only using the ICESat-2 data and the vegetation classification data. First,

considering that the elevation accuracy of terrains provided by ICESat-2 ATL08 products is affected by many factors, we proposed an ICESat-2 terrain control point (TCP) selection criteria to reject the erroneous ICESat-2 terrain points. Then, we generated the correction surface using the interpolation method based on the TCPs. Finally, a corrected SRTM DEM in a forested area was derived through the elevation correction surface.

The method novelty and highlights of this paper are as follows:

1. To the best of our knowledge, we were the first to attempt to correct the elevation error of the SRTM DEM based on the spatial interpolation method using ICESat-2 data.
2. In this study, we developed an ICESat-2 terrain control point selection criteria to obtain high-accuracy TCPs.
3. An easy-to-use method was proposed to correct the elevation error of the SRTM DEM based on the obtained high-accuracy TCPs.

2. Materials

2.1. Test Site

As shown in Figure 1a,b, the test site, located in Massachusetts, USA, has a latitude range of 42° – 43° N, a longitude range of 72° – 73° W, and an elevation range of 0–1094 m. The test site is a typical temperate forest, the main vegetation type is regenerating Eastern Deciduous temperate forest. In addition, the canopy height is mainly concentrated at 20 m. Figure 1b,c also show the datasets used in this study, such as SRTM DEM, ICESat-2 ATL08 products, vegetation classification data, and airborne LiDAR data. Table 1 shows the information about the datasets in this study.

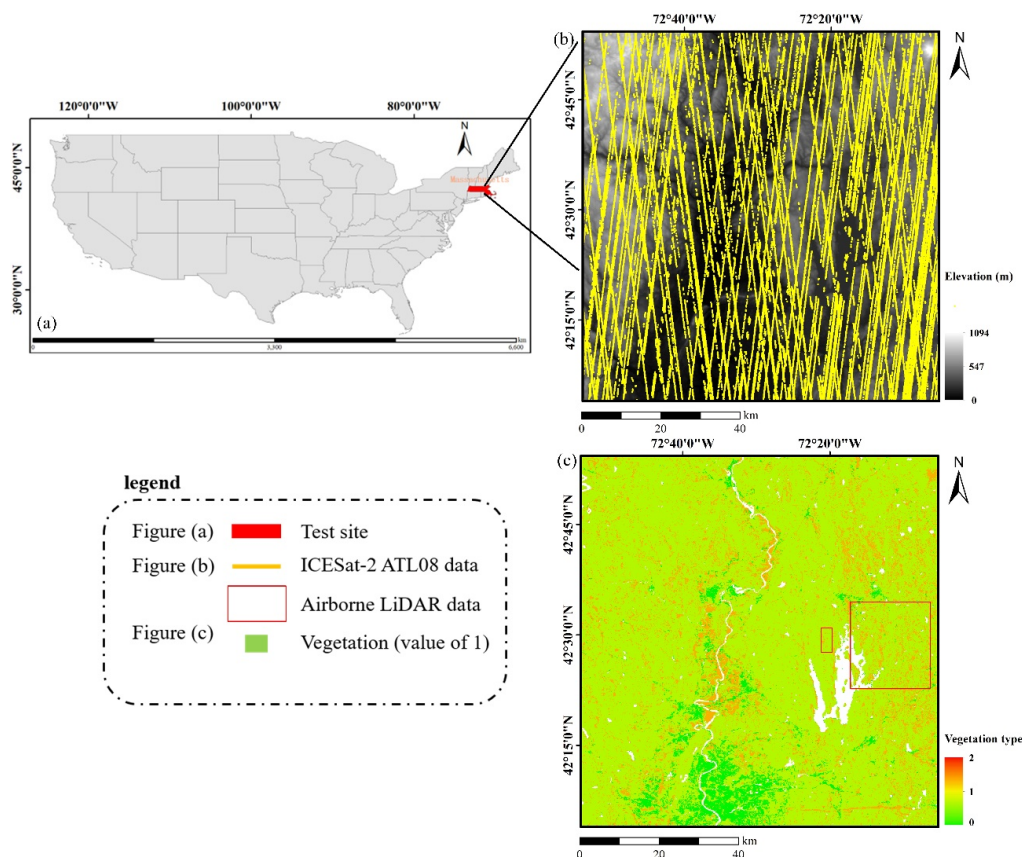


Figure 1. The test site and datasets: (a) the test site; (b) SRTM DEM and ICESat-2 ATL08 data; (c) vegetation classification data and airborne LiDAR data.

Table 1. The information about the datasets used in this study.

Dataset	Resolution (m)	Coordinate System	Elevation Datum	Date (Year)
SRTM	30	WGS—84	EGM96	2014
ICESat-2 ATL08 (version 5)	20	WGS—84	WGS—84	2018–2021
Vegetation Classification data	50	WGS—84	***	2014
The reference LiDAR DTM and CHM	1	UTM	NAVD88	2019

“***” means that the dataset has no definite elevation datum.

2.2. SRTM DEM

The near-global DEM product generated by SRTM has been widely used in many applications. It has a resolution of 30 m and is under the World Geodetic System 1984 (WGS—84) with the 1996 Earth Gravitational Model (Earth Gravitational Model 1996, EGM96) datum [11]. In this study, we used the third edition of the SRTM DEM over the test site, which is available and can be downloaded on the website of the U.S. Geological Survey.

2.3. ICESat-2 ATL08 Product (Version 5)

The ATL08 product is one of the 22 standard products generated by ICESat-2 and is a terrestrial vegetation data product, generated from the ICESat-2 ATL03 photon cloud data product through photon cloud filtering and classification approaches [23]. The ATL08 product provides terrain and forest canopy heights along the track, as well as some related descriptive parameters, including the signal-to-noise ratio, lift rail, cloud cover, etc [24]. These descriptive parameters help in selecting the sampling points of the ATL08 product with higher accuracy. Some detailed descriptions of the ATL08 product can be found in reference [25]. Recent research [23,25,26] verified the subcanopy terrain accuracy of ATL08 products through airborne lidar data, which demonstrated that the terrain results generated by the ICESat-2 ATL08 products have the ability to correct the elevation error of the SRTM DEM in forested areas. The ICESat-2 ATL08 datasets are available from <https://search.earthdata.nasa.gov> (accessed on 1 March 2022).

2.4. Vegetation Classification Data

The TanDEM-X forest/non-forest (FNF) map was introduced as vegetation classification data in this study. It was used to distinguish vegetation and non-vegetation to correct the elevation error of the SRTM DEM. This project was sponsored by the DLR (Microwaves and Radar Institute at the German Aerospace Center). The FNF map has a spatial resolution of 50 m and is available at the following website: <https://download.geoservice.dlr.de/> (accessed on 10 March 2022).

2.5. Airborne LiDAR Data

The airborne LiDAR data were provided by the National Ecological Observatory Network (NEON) in the United States, which was used to generate a high-accuracy digital terrain model (DTM) and canopy height model (CHM) of the study area. The DTM was used to assess the performance of the proposed method. In addition, the CHM was used to analyze the relationship between the accuracy of the error of the SRTM DEM and canopy height. The DTM and CHM derived from airborne LiDAR are projected to the Universal Transverse Mercator (UTM) coordinate system with the North American Vertical Datum of 1988 datum (NAVD88) and stored in TIFF format [27]. With resolutions of 1 m and errors in planimetry and elevation of 0.3 m and 0.5 m, respectively, the lidar DTM and CHM can be downloaded from the NEON official website (<https://www.neonscience.org/> accessed on 4 March 2022).

3. Methods

In general, as shown in Figure 2, the method for the elevation error correction of the SRTM DEM can be divided into three steps: (1) selecting the ICESat-2 terrain control points; (2) interpolating the elevation correction surface of the SRTM DEM and therefore correcting the elevation error of the SRTM DEM; and (3) using the airborne LiDAR-derived DTM and CHM to assess the corrected SRTM DEM. To ensure that the coordinate system and elevation datum of all datasets were consistent, all datasets were projected to the UTM coordinate system, and the elevation datums of all datasets were consistent with EGM96. In addition, all datasets were resampled to the same scale.

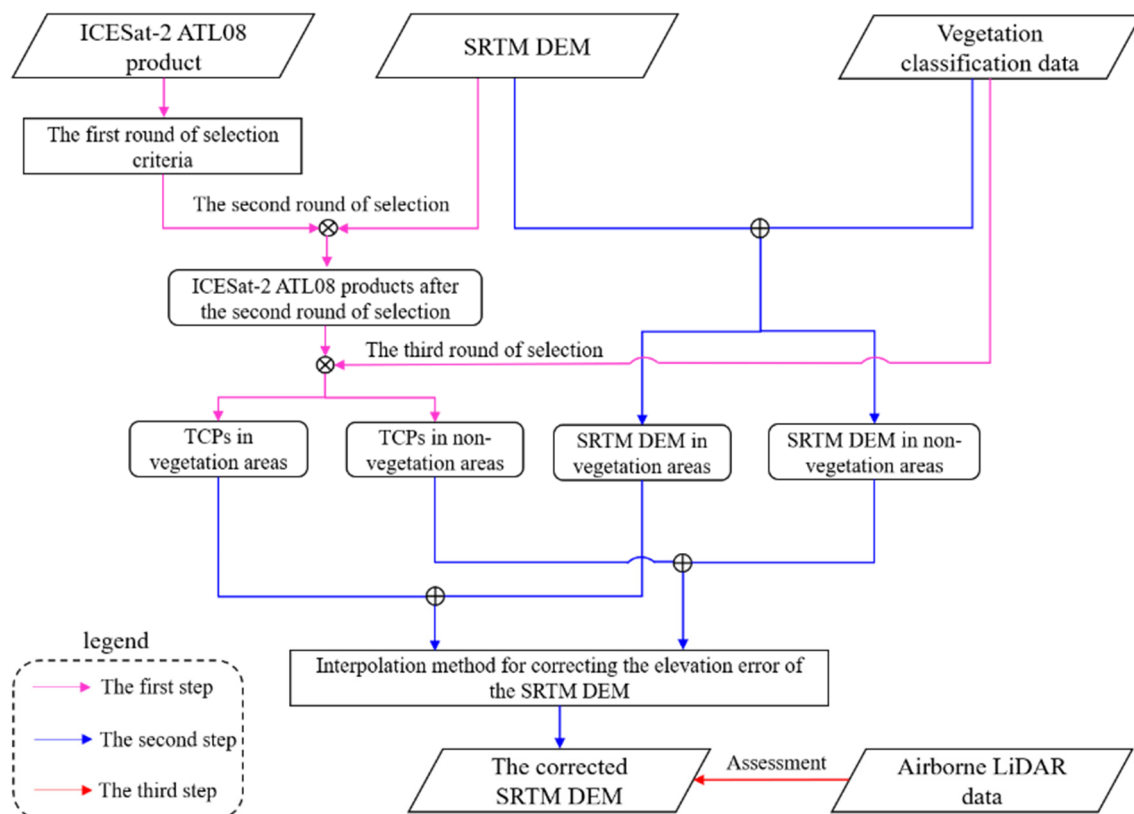


Figure 2. Flow chart of the proposed method.

3.1. The ICESat-2 Terrain Control Points Selecting Criteria

Although NASA provides an amount of ICESat-2 ATL08 products, due to the interference of observation environment error and the processing method, some terrains provided from ICESat-2 ATL08 products have inaccurate elevation values [24]. These erroneous ICESat-2 ATL08 terrains would lead to errors in the SRTM DEM elevation error correction surface directly. Therefore, we proposed three rounds of selection criteria for ICESat-2 ATL08 terrains from three aspects: instrumental and environmental errors, SRTM DEM, and vegetation classification data.

For vegetation areas, due to the influence of canopy coverage, weak beams hardly record complete vegetation and terrain information [26]. Therefore, it is necessary to eliminate ICESat-2 ATL08 products obtained from weak beams according to the parameter description of the satellite's ascending and descending orbit. Additionally, clouds and fog also affect the accuracy of the terrains provided by ICESat-2 ATL08 products, so terrains with a cloud flag (cloud_flag_asr) should be preliminarily eliminated.

After the first round of selection, there are still some terrain outliers provided by ICESat-2 ATL08 products mainly caused by the processing method. Therefore, these terrain outliers should be found under the second round of selection according to the

elevation difference between the elevation of ICESat-2 ATL08 terrains and the SRTM DEM. In vegetation areas, the SRTM DEM elevation represents the phase center height, which is between the subcanopy terrain and the canopy top [11]. The terrains provided by ICESat-2 ATL08 products can more accurately represent the subcanopy terrain, so the elevation of terrains provided by ICESat-2 ATL08 products cannot be higher than the SRTM DEM elevation. In addition, the difference between the SRTM elevation and the ATL08 terrain cannot be higher than the tree height at the corresponding location. According to the above rules, the ICESat-2 ATL08 terrain where the difference between the elevation of the SRTM DEM and that of the ICESat-2 ATL08 terrain is greater than 0 and less than the tree height at the corresponding location can be retained. The tree height can be provided by ICESat-2 ATL08 products according to the tree height field [25].

The accuracy of the SRTM DEM in vegetated areas is much lower than that in non-vegetated areas due to vegetation cover. It should be a large difference between the elevation error correction surface in vegetation areas and non-vegetation areas. Therefore, we derived the third round of selection to classify the terrains provided from ICESat-2 ATL08 products into vegetation and non-vegetation areas by the vegetation classification data. After the above three rounds of selection criteria, we retained higher-precision ICESat-2 terrains named terrain control points (TCPs) for generating elevation correction surfaces of the SRTM DEM.

3.2. Interpolating the Elevation Correction Surface of the SRTM DEM

After selecting the high-precision TCPs provided by ICESat-2 ATL08 products, the elevation error Δh is calculated as the elevation difference between the SRTM DEM and the corresponding TCP.

$$\Delta h = H_{SRTM} - H_{TCP} \quad (1)$$

where H_{SRTM} and H_{TCP} represent the elevation of the SRTM DEM and that of the TCP from ICESat-2 ATL08 products, respectively. According to the first law of geography, everything is related to other things, and similar things are more closely related [28]. Therefore, a continuous elevation error correction surface for the SRTM DEM is derived by the inverse distance weighted (IDW) spatial interpolation method based on some discrete TCPs. The principle of the IDW interpolation method is based on the weighted average of the distances between the TCP and unknown SRTM DEM pixels. The elevation error of the unknown SRTM DEM pixel is calculated based on the IDW interpolation method as follows:

$$err_h_i = \frac{\sum_{j=1}^N \Delta h_j \frac{1}{d_{ij}^k}}{\sum_{j=1}^N \frac{1}{d_{ij}^k}} \quad (2)$$

where err_h_i represents the elevation error of the unknown SRTM DEM pixel i and Δh_j represents the elevation error of the SRTM DEM pixel at TCP j . d_{ij}^k represents the distance between the unknown SRTM DEM pixel i and TCP j , which can be demonstrated as the weight of TCP j . N is the number of TCPs, and k is the power of distance. We set k to 2 in this study.

The elevation error of the SRTM DEM is quite different between the vegetation area and the non-vegetated. Therefore, the SRTM DEM pixels in vegetation areas should be interpolated by TCPs in vegetation areas, and the SRTM DEM pixels in non-vegetated areas should be interpolated by TCPs in non-vegetated areas. The vegetation attributes of the SRTM DEM pixels can be provided by vegetation classification data in this study. Overall, the elevation correction surface of the SRTM DEM is obtained by traversing all unknown SRTM DEM pixels using the proposed method. Eventually, the corrected SRTM DEM can be obtained by subtracting the elevation correction surface from the SRTM DEM.

3.3. Assessment

To evaluate the corrected SRTM DEM, the elevation residuals between the corrected SRTM DEM and the reference LiDAR DTM were calculated. Based on the elevation residuals, four precision statistical values, including the mean error (mean), standard deviation (std), coefficient of determination (R-square, R^2), and root mean square error (RMSE), were calculated to evaluate the accuracy of the corrected SRTM DEM. In addition, we used the LiDAR CHM to analyze the relationship between the accuracy of the error of the SRTM DEM and canopy height.

4. Results

4.1. Accuracy of the TCPs

To illustrate the importance of the TCPs selection, the final selected TCPs and terrains after the first round of selection were compared with the corresponding elevations extracted from LiDAR DTM. Table 2 shows the results that the terrain results for each round of selection. For the original terrain points, there are some invalid values. In addition, terrain points provided by weak beams are often inaccurate in forested areas, which need to be screened out. After the first round of selection, 571,514 terrain points were retained with an elevation range of -300 – 1000 m. The remaining terrain points after the first round of selection yield a low RMSE of 2.05 m. However, there may be still some terrain outliers mainly caused by the processing method need to be filtered out. Table 2 shows that there are 452,268 terrain points with an elevation range between -30 and 1100 m remained. The remaining terrain points after the second round of selection yield an RMSE of 1.03 m. The terrain points after the second round of selection are actually TCPs. The histogram of errors in the terrains after only the first-round selection and the TCPs are shown in Figure 3. It can be observed that the terrain accuracy of TCPs is nearly 50% higher than the terrain after only the first-round selection. The purpose of the third round of selection was to classify TCPs into vegetated and non-vegetated areas. It can be found in Table 2 that the number of TCPs in vegetated areas is higher than that in non-vegetated areas (Table 2). The TCPs in non-vegetated areas have a small RMSE of 0.68 m. Although the RMSE of the TCPs in the vegetated areas is higher than that in the non-vegetation areas, it is acceptable. The elevation range of TCPs is similar to that of the SRTM DEM, which indicates that the TCPs after three rounds of selection are evenly distributed in the test site. In general, it can be concluded that the proposed selection criteria are reliable and reject many ICESat-2 terrains with a large error.

Table 2. The results for each round of selection.

	Number of the Terrain Points		RMSE (m)		Elevation Range (m)	
The original terrain points	868,543		***		***	
The first round of selection	571,514		2.05		-300 – 1100	
The second round of selection	452,268		1.03		-30 – 1100	
The third round of selection	Veg	Non-Veg	Veg	Non-Veg	Veg	Non-Veg
	385,347	66,921	1.03	0.68	-20 – 1000	-30 – 1100

“***” means no definite value because there are some invalid values in the original ATL08 terrain product. Veg and Non-Veg represent vegetation areas and non-vegetation areas, respectively.

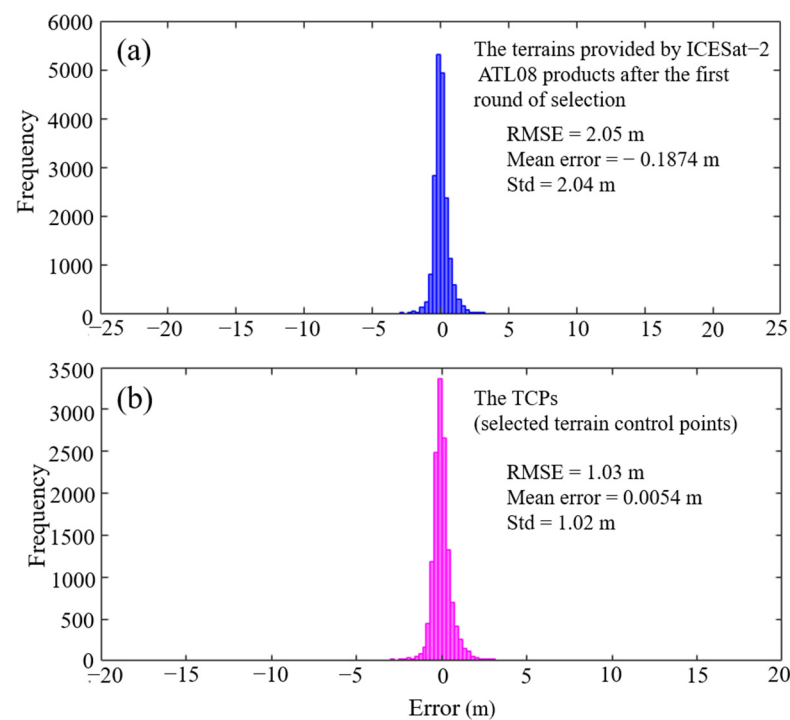


Figure 3. (a) Histogram of elevation differences between the terrain models provided by ICESat-2 ATL08 products and the reference DTM; and (b) histogram of errors between the TCPs and the reference DTM.

4.2. The Accuracy of the Corrected SRTM DEM

The accuracy of the original and corrected SRTM DEMs are assessed against the reference LiDAR DTM, using some indices, including RMSE, R^2 , mean error, and standard deviation, as shown in Figure 4. Figure 4a,b shows that the corrected SRTM DEM and original SRTM DEM achieve RMSEs of 4.2 m and 9.8 m, as well as R^2 values of 99% and 96%, respectively. Compared with the original SRTM DEM, there is a significant improvement in the corrected SRTM DEM. The corrected SRTM DEM has a 57% improvement in terrain accuracy compared to the original SRTM DEM. In addition, the histogram of errors between the corrected SRTM DEM/original SRTM DEM and the reference LiDAR DTM is shown in Figure 4c. It can be observed that there is an overall shift of the elevation errors between the corrected SRTM DEM and DTM, resulting in a very low mean error value close to 0. Although the standard deviation (Std) of the elevation errors declined by only 0.2 m, it can be speculated that some errors may exist in the vegetation classification data, and some attribute features of the SRTM DEM were not considered in this study. The improvement in the corrected SRTM DEM can also be found in a qualitative evaluation, as shown in Figure 5. A smooth corrected SRTM DEM (Figure 5a) and other detailed information (Figure 5b–e) are presented. The fact that the corrected SRTM DEM is more consistent with the reference high-precision LiDAR DTM than the original SRTM DEM is shown in Figure 5b–d. It can be concluded that the proposed method effectively corrected the elevation error caused by the canopy cover in the forested areas of the SRTM DEM. Figure 5e also verifies our conclusion. The represented profile shows that the corrected SRTM DEM is closer to the DTM, and the original SRTM DEM has an obvious overestimation in the vegetation areas. Although the corrected SRTM DEM has a minor amount of underestimation, it shows good consistency with the DTM in general. These underestimated areas may be influenced by errors in the vegetation classification data due to the acquisition time, resulting in bare areas being treated as vegetation areas.

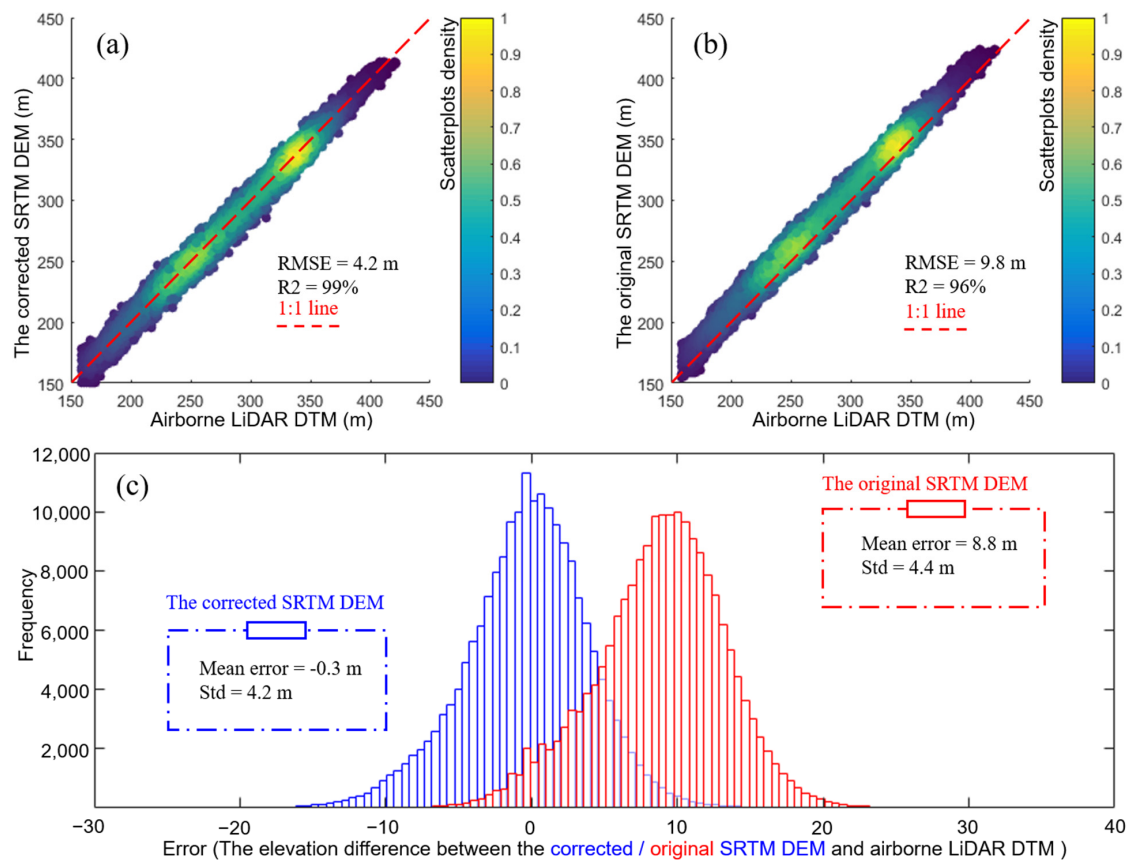


Figure 4. Scatterplots of (a) the corrected SRTM DEM and (b) original SRTM DEM versus the reference LiDAR DTM; (c) histogram of errors between the corrected SRTM DEM/original SRTM DEM and the reference LiDAR DTM.

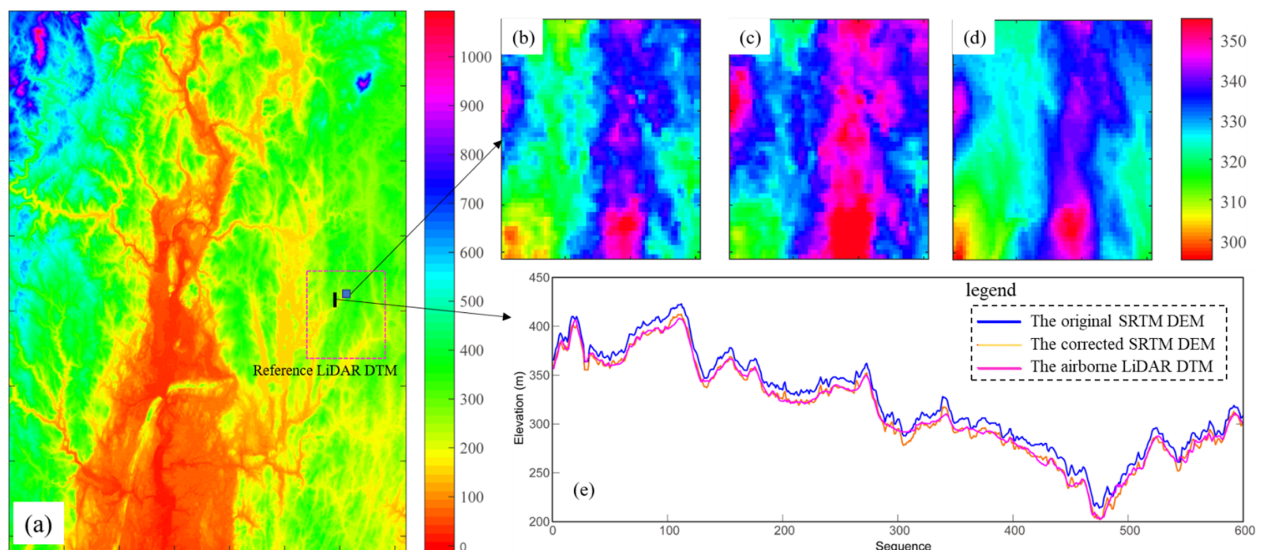


Figure 5. Qualitative evaluation of the corrected SRTM DEM. (a) The corrected SRTM DEM; partially enlarged views of (b) the corrected SRTM DEM, (c) the original SRTM DEM and (d) the reference LiDAR DTM; (e) profiles compare the terrains of the corrected SRTM DEM, the original SRTM DEM, and the reference LiDAR DTM.

5. Discussion

The accuracy of the corrected SRTM DEM derived by the proposed method in forested areas is influenced by some error factors, such as the accuracy of the vegetation classification data, slope, and forest canopy height [15].

Since the acquisition time of vegetation classification data may be inconsistent with SRTM DEM and ICESat-2, there may be some errors in vegetation classification data due to some external factors, such as some forests being destroyed, returning farmland to forests, etc. This would lead to some errors in some local areas due to misclassified vegetation areas or non-vegetation areas. Therefore, it is important to choose vegetation classification data that are temporally consistent with SRTM DEM and ICESat-2. In the future, we will generate time-sensitive vegetation classification data using a large number of optical images.

We also explore the effect of other factors on the corrected SRTM DEM and the original SRTM DEM, including the slope and canopy height. As shown in Figure 6, we divide the error factors in the test site into five groups and calculate the RMSE of the corrected SRTM DEM and the original SRTM DEM. Figure 6a shows that with increasing slopes, the accuracy of the corrected SRTM DEM and the original SRTM DEM decreases. The reason is that the interferogram has a low coherence in areas with large slopes, so the error of the original SRTM will increase with increasing slope [10]. However, the proposed method does not take the effect of the slope into account when correcting the elevation error of the SRTM DEM in forested areas. For the canopy height error factor, the RMSE of the original SRTM DEM increases when the canopy height increases, which can be attributed to the fact that the phase center height increases with tree height (Figure 6b). However, the corrected SRTM shows a different phenomenon. The RMSE of the corrected SRTM DEM increases as the canopy height increases when the canopy height is larger than 10 m (Figure 6b). Additionally, the RMSE of the corrected SRTM DEM with a canopy height below 10 m is higher than that with a canopy height of 10–30 m, especially the terrain accuracy, which is the lowest in non-vegetation areas (Figure 6b). It can be inferred that the inconsistency with the SRTM DEM and ICESat-2 results in low accuracy of the SRTM DEM in bare land. In the future, we will use an Artificial Neural Network approach [28] that fully considers the attribute features (slope, canopy height, canopy cover, etc.) to correct the elevation error of the SRTM DEM in forested areas. In addition, we plan to correct the national-scale SRTM DEM in forested areas using an enhanced interpolation method that considers attribute features (slope, canopy height, canopy cover, etc.).

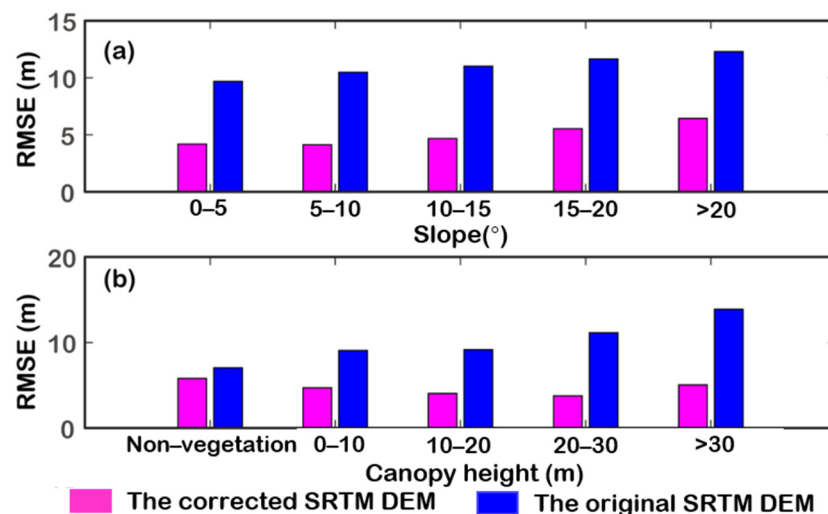


Figure 6. The relationship between the RMSE value of the corrected/original SRTM DEM and (a) slope and (b) canopy height.

6. Conclusions

In this study, we generated an elevation correction surface to correct the elevation error of the SRTM DEM. To the best of our knowledge, we were the first to use ICESat-2 data and vegetation classification data based on an elevation correction surface interpolation method to correct the elevation error of the SRTM DEM in forested areas. It can be illustrated from the accuracy of TCPs that the three rounds of selection for the terrains provided by ATL08 are necessary, which directly improves the accuracy of the elevation correction surface. Moreover, the results show that the proposed method significantly improves the accuracy of the SRTM DEM in forested areas. It can be concluded that the proposed method can effectively eliminate the elevation error of the SRTM DEM.

We also found that the accuracy of vegetation classification data directly affects the corrected SRTM DEM on a local scale. This study suggests that it is important to choose vegetation classification data that are temporally consistent with the SRTM DEM and ICESat-2. We will make more attempts in generating vegetation classification data that are largely temporally consistent with the SRTM DEM and ICESat-2 in future work. In addition, the corrected SRTM DEM and original SRTM DEM are sensitive to some attribute features, which means that the accuracy of the corrected SRTM DEM can be improved by considering these attribute features. Therefore, to correct the elevation error of the SRTM DEM accurately, some attribute features, such as slopes, canopy heights, canopy covers, etc., will be considered to improve the interpolation method in our future work.

Author Contributions: Conceptualization, Y.L., H.F. and J.Z.; methodology, Y.L., H.F., P.Y. and K.W.; validation, Y.L., H.F., P.Y., K.W. and L.W.; formal analysis, Y.L., H.F. and J.Z.; investigation, Y.L., L.W. and J.Z.; resources, Y.L., H.F., P.Y., K.W. and L.W.; data curation, Y.L., H.F., J.Z. and S.G.; writing—original draft preparation, Y.L.; writing—review and editing, Y.L., H.F., P.Y., K.W., L.W. and S.G.; visualization, Y.L., P.Y. and L.W.; supervision, H.F. and J.Z.; project administration, H.F. and J.Z.; funding acquisition, J.Z., H.F., Y.L. and S.G. All authors have read and agreed to the published version of the manuscript.

Funding: This research was partly funded by the National Natural Science Foundation of China, grant numbers 41820104005, 42030112, and 41904004. Additionally, this research was partly funded by the Natural Science Foundation of Hunan Province of China (grant number, 2021JJ30808), the Changsha Municipal Natural Science Foundation (grant number, kq2202111), and the Fundamental Research Funds for the Central Universities of Central South University (grant number, 506021729). The APC was funded by the National Natural Science Foundation of China, grant number 41820104005.

Data Availability Statement: The SRTM DEM is available from USGS.gov | Science for a changing world. The ICESat-2 ATL08 datasets are available from <https://search.earthdata.nasa.gov/search> (accessed on 1 March 2022). The vegetation classification data are available from EOC Download—FNF50 (dlr.de) (accessed on 10 March 2022). The airborne LiDAR data can be found on the NEON official website <https://www.neonscience.org/> (accessed on 4 March 2022).

Acknowledgments: Many thanks to NASA, USGS, DLR, and NEON for providing free datasets.

Conflicts of Interest: The authors declare no conflict of interest.

References

1. Sun, Q.; Zhang, L.; Ding, X.L.; Hu, J.; Li, Z.W.; Zhu, J.J. Slope deformation prior to Zhouqu, China landslide from InSAR time series analysis. *Remote Sens. Environ.* **2015**, *156*, 45–57. [\[CrossRef\]](#)
2. Zhao, R.; Li, Z.W.; Feng, G.C.; Wang, Q.J.; Hu, J. Monitoring surface deformation over permafrost with an improved SBAS-InSAR algorithm: With emphasis on climatic factors modeling. *Remote Sens. Environ.* **2016**, *184*, 276–287. [\[CrossRef\]](#)
3. Rajendran, S.; Nasir, S. ASTER capability in mapping of mineral resources of arid region: A review on mapping of mineral resources of the Sultanate of Oman. *Ore Geol. Rev.* **2019**, *108*, 33–53. [\[CrossRef\]](#)
4. Rajendran, S.; Nasir, S.; El-Ghali, M.A.K.; Alzebedah, K.; Salim Al-Rajhi, A.; Al-Battashi, M. Spectral Signature Characterization and Remote Mapping of Oman Exotic Limestones for Industrial Rock Resource Assessment. *Geosciences* **2018**, *8*, 145. [\[CrossRef\]](#)
5. Wang, Y.; Dong, P.; Liao, S.; Zhu, Y.; Zhang, D.; Yin, N. Urban Expansion Monitoring Based on the Digital Surface Model—A Case Study of the Beijing–Tianjin–Hebei Plain. *Appl. Sci.* **2022**, *12*, 5312. [\[CrossRef\]](#)
6. McGowan, S.; Leavitt, P.R.; Hall, R.I.; Wolfe, B.B.; Edwards, T.; Karst-Riddoch, T.; Vardy, S.R. Interdecadal declines in flood frequency increase primary production in lakes of a northern river delta. *Glob. Chang. Biol.* **2011**, *17*, 1212–1224. [\[CrossRef\]](#)

7. Ludwig, R.; Schneider, P. Validation of digital elevation models from SRTM X-SAR for applications in hydrologic modeling. *ISPRS J. Photogramm. Remote Sens.* **2006**, *60*, 339–358. [\[CrossRef\]](#)
8. Lei, Y.; Paul, S. An Automatic Mosaicking Algorithm for the Generation of a Large-Scale Forest Height Map Using Spaceborne Repeat-Pass InSAR Correlation Magnitude. *Remote Sens.* **2015**, *7*, 5639–5659. [\[CrossRef\]](#)
9. Steelman, T.A.; Maguire, L.A. Understanding participant perspectives: Q-methodology in national forest management. *J. Policy Anal. Manag.* **1999**, *18*, 361–388. [\[CrossRef\]](#)
10. Farr, T.G.; Rosen, P.A.; Caro, E.; Crippen, R.; Duren, R.; Hensley, S.; Kobrick, M.; Paller, M.; Rodriguez, E.; Roth, L. The Shuttle Radar Topography Mission. *Rev. Geophys.* **2007**, *45*, 361. [\[CrossRef\]](#)
11. Rabus, B.; Eineder, M.; Roth, A.; Bamler, R. The shuttle radar topography mission—A new class of digital elevation models acquired by spaceborne radar. *ISPRS J. Photogramm. Remote Sens.* **2003**, *57*, 241–262. [\[CrossRef\]](#)
12. Falorni, G.; Teles, V.; Vivoni, E.R.; Bras, R.L.; Amaratunga, K.S. Analysis and characterization of the vertical accuracy of Digital Elevation Models from the Shuttle Radar Topography Mission. *J. Geophys. Res. Atmos.* **2005**, *110*, F02005. [\[CrossRef\]](#)
13. Casu, F.; Manzo, M.; Lanari, R. A quantitative assessment of the SBAS algorithm performance for surface deformation retrieval from DInSAR data. *Remote Sens. Environ.* **2006**, *102*, 195–210. [\[CrossRef\]](#)
14. Farr, T.G.; Kobrick, M. Shuttle radar topography mission produces a wealth of data. *Eos Trans. Am. Geophys. Union* **2013**, *81*, 583–585. [\[CrossRef\]](#)
15. Su, Y.; Guo, Q.; Ma, Q.; Li, W. SRTM DEM Correction in Vegetated Mountain Areas through the Integration of Spaceborne LiDAR, Airborne LiDAR, and Optical Imagery. *Remote Sens.* **2015**, *7*, 11202–11225. [\[CrossRef\]](#)
16. Su, Y.; Guo, Q. A practical method for SRTM DEM correction over vegetated mountain areas. *ISPRS J. Photogramm. Remote Sens.* **2014**, *87*, 216–228. [\[CrossRef\]](#)
17. Zhao, X.; Su, Y.; Hu, T.; Chen, L.; Gao, S.; Wang, R.; Jin, S.; Guo, Q. A global corrected SRTM DEM product for vegetated areas. *Remote Sens. Lett.* **2018**, *9*, 393–402. [\[CrossRef\]](#)
18. O’Loughlin, F.E.; Paiva, R.C.D.; Durand, M.; Alsdorf, D.E.; Bates, P.D. A multi-sensor approach towards a global vegetation corrected SRTM DEM product. *Remote Sens. Environ.* **2016**, *182*, 49–59. [\[CrossRef\]](#)
19. Arefi, H.; Reinartz, P. Accuracy Enhancement of ASTER Global Digital Elevation Models Using ICESat Data. *Remote Sens.* **2011**, *3*, 1323–1343. [\[CrossRef\]](#)
20. Neuenschwander, A.; Pitts, K. The ATL08 land and vegetation product for the ICESat-2 Mission. *Remote Sens. Environ.* **2019**, *221*, 247–259. [\[CrossRef\]](#)
21. Li, Y.; Zhu, J.; Fu, H.; Gao, S.; Wang, C. Filtering Photon Cloud Data in Forested Areas Based on Elliptical Distance Parameters and Machine Learning Approach. *Forests* **2022**, *13*, 663. [\[CrossRef\]](#)
22. Zhu, J.; Yang, P.; Li, Y.; Xie, Y.; Fu, H. Accuracy assessment of ICESat-2 ATL08 terrain estimates: A case study in Spain. *J. Cent. South Univ.* **2022**, *29*, 226–238. [\[CrossRef\]](#)
23. Ice, Cloud, and Land Elevation Satellite-2 (ICESat2) Algorithm Theoretical Basis Document (ATBD) for Land-Vegetation Along-Track Products (ATL08). pdf. Available online: <https://icesat-2.gsfc.nasa.gov/science/data-products> (accessed on 1 March 2022).
24. Neuenschwander, A.; Guenther, E.; White, J.C.; Duncanson, L.; Montesano, P. Validation of ICESat-2 terrain and canopy heights in boreal forests. *Remote Sens. Environ.* **2020**, *251*, 112110. [\[CrossRef\]](#)
25. Neuenschwander, A.L.; Magruder, L.A. Canopy and Terrain Height Retrievals with ICESat-2: A First Look. *Remote Sens.* **2019**, *11*, 1721. [\[CrossRef\]](#)
26. Kampe, T.U.; Johnson, B.R.; Kuester, M.A.; Keller, M. NEON: The first continental-scale ecological observatory with airborne remote sensing of vegetation canopy biochemistry and structure. *J. Appl. Remote Sens.* **2010**, *4*, 043510. [\[CrossRef\]](#)
27. Tobler, W.R. A Computer Movie Simulating Urban Growth in the Detroit Region. *Econ. Geogr.* **1970**, *46*, 234–240. [\[CrossRef\]](#)
28. Kim, D.E.; Liu, J.; Liong, S.Y.; Gourbesville, P.; Strunz, G. Satellite DEM Improvement Using Multispectral Imagery and an Artificial Neural Network. *Water* **2021**, *13*, 1551. [\[CrossRef\]](#)